wjert, 2019, Vol. 5, Issue 2, 168-186. Original Article ISSN 2454-695X

World Journal of Engineering Research and Technology
WJERT
www.wjert.org
SJIF Impact Factor: 5.218

ENERGY MANAGEMENT OF SOLAR THERMAL ENERGY DRIVING ORC AND TDC

K. A. Abed*[1], Amr M. A. Amin[2], Adel A. El-Samahy[2] and Abdullah M. A. Shaaban[1]

[1]Mechanical Eng. Depart., National Research Centre (NRC).

[2]Electrical Eng. Depart., Faculty of Engineering, Helwan University.

Article Received on 03/01/2019 **Article Revised on 24/01/2019** **Article Accepted on 15/02/2019**

***Corresponding Author**
K. A. Abed
Mechanical Eng. Depart., National Research Centre (NRC).

ABSTRACT

The present work aims to manage the thermal energy stored from concentrated solar power (CSP) research plant, in order to obtain the best operating condition of CSP system. This plant consists of solar collector field of 120 kW peak thermal capacity, thermal storage tank with 3 tons of therminol-66 oil, an organic rankine cycle (ORC) of 8 kW nominal electric power production capacity, and thermally driven absorption chiller (TDC) of 35 kW cooling capacity. The system was modeled mathematically then calculated using engineering equation solver (EES) software in order to analyze the performance at similar conditions to the real ones to ensure the feasibility of the presented study. When increasing the input thermal power for both ORC and TDC, the kWh cost decreases. The lowest price for ORC kWh is 1.131 $/kWh when 100% of the stored thermal power is used by ORC to generate electricity. Also, the lowest price for TDC kWh is 0.1214 $/kWh when 100% of the stored thermal power is directed to the TDC. To compromise between both ORC and TDC, The best operating condition is obtained when about 45.83% from stored thermal power is used for ORC and 54.17% is used for TDC. In this case, the cost of electrical kWh from ORC is about 1.26 $, while the cost of refrigerant kWh from TDC is about 0.126 $.

KEYWORDS: Renewable Energy, Concentrated Solar Power System, Organic Rankine Cycle, Thermally Driven Absorption Chiller.

INTRODUCTION

Nowadays, energy is one of the most basic and crucial elements upon which to base a life and an economy. Energy is very important for daily tasks in homes, schools, hospitals, business, transport applications, industries and countless other places. Most of energies come from burning fossil fuels like oil, coal and natural gas which are called conventional or traditional energy resources.[1] Since crisis for USA of the mid 1970's, the world's industrialized nations look at renewable energy sources (RES) as a supplement to providing the projected increase in energy demand in their nations in addition to increase awareness of the effects of emissions from fossil fuel power plants to the humans and environment. Governments in industrial countries are currently made debating and enacting pollution control regulations into laws.[2]

Solar energy is a source, which can be exploited in two main ways to generate power: direct conversion into electric energy using photovoltaic (PV) panels and by means of a thermodynamic cycle. In CSP plants it is the sun's thermal energy to be stored, whereas in PV applications it is the electrical energy to be stored in batteries. Umberto Desideri et al studied the performance of concentrated solar power plants equipped with molten salts thermal storage to cover a base load of 3 MWe. The electricity production of the CSP facilities has been analyzed and then compared with the electricity production of PV plants.[3]

Wisam Abed et al presented a detail dynamic model of a 50 MWe parabolic trough power plant.[4] The parabolic trough power plant is modeled using advanced process simulation software (APROS). During summer days, the plant typically operates for 10–12 hr a day on solar energy at full-rated electric output. Furthermore, the thermal storage system enables the parabolic trough power plant to produce a constant electrical power rate, despite the slight fluctuations in the solar radiation. The thermal storage system after sunset continues approximately 7.5 hr for covering electrical power of 48 MWe until the thermal storage energy is completely depleted.

Monica Borunda et al presented a study of a small CSP plant coupled to an ORC with thermal energy storage.[5] Molten salts could be a very good possibility to highly increase the solar fraction but it is much more expensive. On the other hand concrete storage is much cheaper but with less heat capacity. However phase change materials may be a good and interesting candidate with a balanced compromise between heat capacity and price.

Rady et al studied a small scale multi-generation solar plant which consists of solar collector field, thermal storage tank, an ORC, and TDC.[10] This article reported on the plant layout, thermodynamic analysis, solar field design, ORC and TDC integration, thermal storage system, and control system and operation strategy. The plant is modeled and analyzed using parabolic trough (PTC) and Linear Fresnel collectors (LFR) at different operation modes in typical winter and summer days. The use of LFR solar collectors results in reduction in the operation hours of ORC and TDC by about 50% and 30%, respectively.

Mohamed H. Ahmed et al also studied solar power plant consisting of ORC and absorption chiller.[7] This paper presented a numerical simulation for the performance of solar thermal power plant which consists of 190 m2 of concentrated PTC with a storage tank and an ORC. A study of the operating parameters of the PTC performance was presented in this paper. The plant used the Therminol-VP1 as a storage media and also as a heat transfer fluid with flow rate ranges from 0.9 to 1.8 kg/s for the solar collectors. It's used also as a heat source for the ORC and the absorption chiller with a flow rate range from 0.3 to 0.9 kg/s. The model studied also the effect of these operating modes on the plant performance. The simulation model proves that the PTC produces a maximum thermal power of about 70 and 115 kW in winter and summer respectively.

Mustapha Merzouk et al studied the performance of a single effect solar absorption cooling system.[6] A dynamic simulation model, for a solar powered absorption cooling system was developed, and validated using measured data. Yeung et al, designed and installed a solar driven absorption chiller at the University of Hong Kong, this system included 4.7 kW absorption chiller, flat plate solar collectors with a total area of 38.2 m², water storage tank and the rest of the equipment. They reported that the collector efficiency was estimated at 37.5%, the annual system efficiency at 7.8% and an average solar fraction of 55%, respectively. In 2012 Rosiek, evaluated the performance of a solar-assisted 70 kW single effect LiBr-Water chiller located in Spain and achieved a maximum COP of 0.6 and Ali, assessed the performance of a 35 kW solar absorption cooling plant and reported maximum collectors' field efficiency of 49.2% and a COP of 0.81. Hammad and Zurigat, described the performance of a 1.5 Ton solar cooling unit. The unit comprises a 14 m² flat plate solar collector system and five shell and tube heat exchangers. The unit was tested in April and May in Jordan. The maximum value obtained for actual coefficient of performance was 0.85.

In 2013, G. Cascales, studied the global modeling of an absorption system working with LiBr/H2O assisted by solar energy.

From the previous survey which includes some of the prior art for the work on concentrated solar power and storage the collected thermal energy to produce electrical power or for cooling load. Most studies work about either concentrated solar power in general or one of the electricity generation by ORC and cooling by absorption chiller. Concentrated solar power system which contains thermal energy storage system, organic rankine cycle, and thermal absorption chiller is very important. So, the present work aims to get the mathematical modeling of the system and simulating it on EES software.

A schematic of the solar power plant using the organic rankine cycle for electric generation and an absorption chiller for air conditioning purpose is shown in figure 1. The main purpose from this plant is the scientific research and studying the performance of the plant. The main parts of the plant are the solar collector field, storage tank, the organic rankine cycle, and absorption chiller.

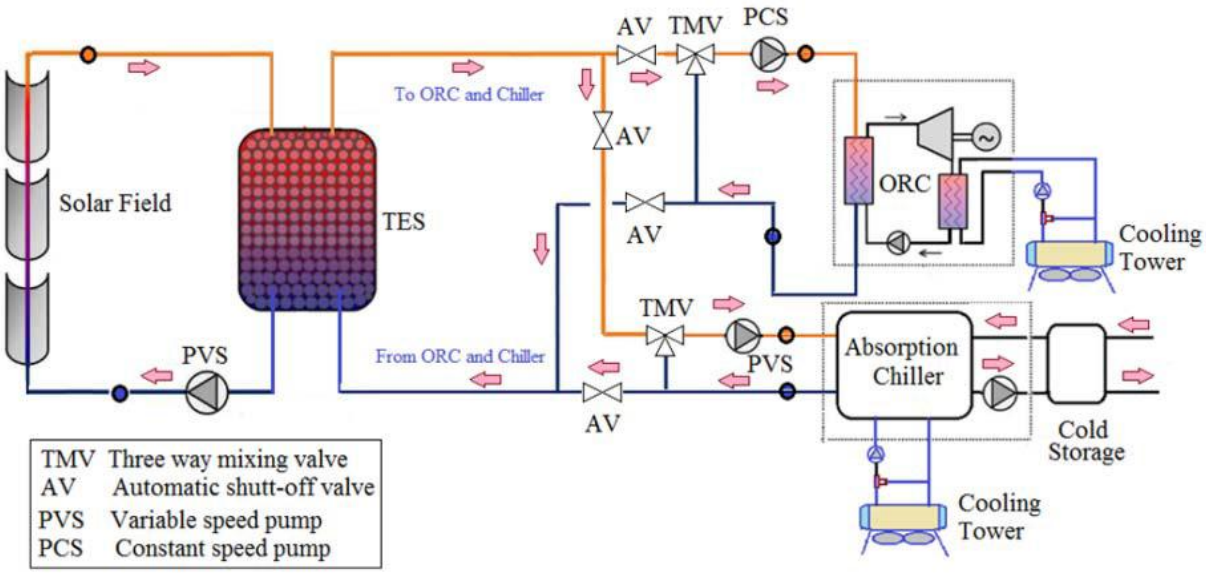

Fig. 1: Schematic diagram of the system.

2. Mathematical Modeling of the System

Mathematical modeling is a representation in mathematical terms of the behavior of real devices and objects we want to know how to make or generate mathematical representations or models, how to validate them, how to use them, and how and when their use is limited. Since the modeling of devices and phenomena is essential to both engineering and science,

engineers and scientists have very practical reasons for doing mathematical modeling. In addition, engineers, scientists, and mathematicians want to experience the sheer joy of formulating and solving mathematical problems.

2.1. Organic Rankine Cycle Modeling

The organic Rankine cycle is consists of an evaporator, a condenser, a pump and a turbine. From state 1 to 2, an ideal pump executes an adiabatic, reversible (isentropic) process to raise the working fluid from the condenser pressure to the evaporator pressure. From state 2 to state 3, an evaporator heats the fluid at a constant pressure (isobar transformation) moving from a saturated liquid state 2' to a saturated vapor state 3' where all the liquid becomes vapor. Then the fluid is superheated until it reaches the state 3. After, the superheat vapor fluid enters in a turbine where it produces expansion through an adiabatic and reversible process. The superheat process is necessary in order to guarantee that in the turbine only vapor is present, this preserving the turbine blades from condensation and erosion. However, the amount of superheat should be kept as low as possible in order to avoid waste of energy and maximize the performance of the entire cycle. The typically used working fluid is an organic fluid which is characterized by low latent heat and high density. These properties are useful to increase the turbine inlet mass flow rate. Common working fluids that can be used are R-123, R-134a and R-245fa. The properties of the working fluid have a significant impact on the performance of the ORC cycle. The appropriate working fluids properties can lead to a higher cycle performance.[7]

Modeling of the ORC is based on modeling of all components forming the cycle as shown in figure 2. The evaporator and the condenser were treated as a heat exchanger. The turbine and pump were simulated with isentropic process the components parameters were selecting for the available component in the market.

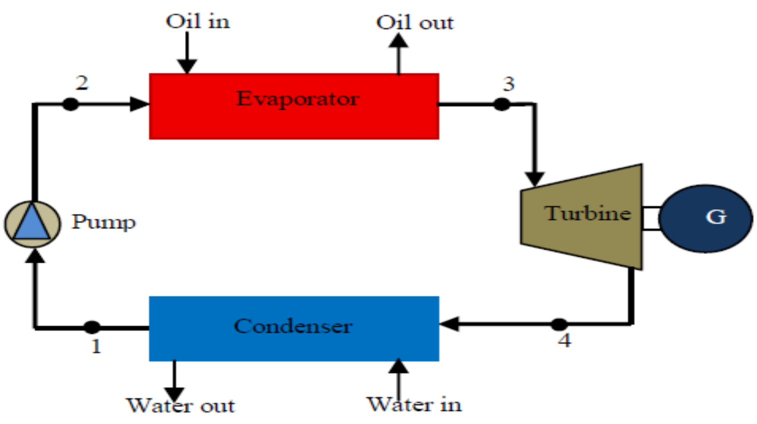

Fig. 2: Schematic diagram of the storage tank with segments.[7]

One-dimensional heat transfer was assumed between the two heat transfer fluids. The thermal oil represents the heating source fluid which flow in the evaporator as one phase flow, while the organic fluid represents the cold fluid and pass through the evaporator in the different three phases (liquid, two phase and vapor phase). So that, the evaporator was divided to three main sections which are the liquid, two phase and the vapor sections each section was related as a separated heat exchanger. As heat losses in heat exchangers are neglected, the amount of the heat added to the working fluid in time is equal to the heat extracted from the heat source.

In general, for each zone the inlet temperature for the hot and the cold fluid stream are $T_{h,i}$ and$T_{c,i}$, respectively, and the outlet temperature for hot and cold streams are $T_{h,o}$ and $T_{c,o}$, respectively. The outlet fluids temperatures were calculated from the following equation.[7]

$$Q = \dot{m}_h Cp_h (T_{h,i} - T_{h,o}) = \dot{m}_c Cp_c (T_{c,o} - T_{c,i}) \quad \ldots\ldots (1)$$

Where:

Q: The actual heat transfer rate (kW).

$\dot{m}_h$: The mass flow rates of the hot fluid (kg/s)

$\dot{m}_c$: The mass flow rates of the cold fluid (kg/s)

Cp_h: The specific heat of the hot fluid (kJ/kg k)

Cp_c: The specific heat of the hot fluid (kJ/kg k)

The working fluid heated in the evaporator to superheated vapor at constant pressure (evaporating pressure). The heat transfer rate from the evaporator (Q_e) into the working fluid is given by:

$$Q_e = \dot{m_f}(h_3 - h_2) = \dot{m_f} Cp_f (T_3 - T_2) \quad \text{..... (2)}$$

Where,

$\dot{m_f}$: is the mass flow rate of the working fluid (kg/s)

h_3, h_2: is the enthalpy at points 3 and 2 (kJ/kg)

T_3, T_2: is the Temperature degree at points 3 and 2 (K)

Cp_f: is the specific heat of the working fluid (kJ/kg K)

The superheated vapor working fluid passes through the turbine to generate the mechanical power. Firstly, we can calculate the enthalpy at point 4 from the following equation (Assume Isentropic):

$$\eta_{turbine} = \frac{h3-h4}{h3-h4s} = \frac{T3-T4}{T3-T4s} \quad \text{..... (3)}$$

Where,

$\eta_{turbine}$: is the turbine efficiency

h_4: is the actual enthalpy at (kJ/kg)

T_4: is the actual Temperature degree at (K)

h_{4s}: is the isentropic enthalpy at (kJ/kg)

T_{4s}: is the isentropic Temperature degree at (K)

Then, the power output from the (W_t) turbine is given by:

$$W_t = \dot{m_f}(h_3 - h_4) = \dot{m_f} Cp_f (T_3 - T_4) \quad \text{..... (4)}$$

The exhaust vapor exits the turbine to the condenser where it is condensed by cooling water. The heat rate removed by the condenser (Q_c) can be expressed as:

$$Q_c = \dot{m_f}(h_4 - h_1) = \dot{m_f} Cp_f (T_4 - T_1) \quad \text{..... (5)}$$

Where,

h_1: is the enthalpy at point 1(kJ/kg)

T_1: is the temperature at point 1 (K)

The pump power (Wp) can be expressed as: (Assume Isentropic)

$$W_p = \dot{m_f}(h_2 - h_1) = \dot{m_f} Cp_f (T_2 - T_1) \quad \text{..... (6)}$$

To get the pump efficiency η_{pump}

$$W_p \cong \dot{m_f} \frac{\upsilon_1 \Delta P}{\eta_{pump}} \cong \dot{m_f} \frac{\upsilon_1 (P2 - P1)}{\eta_{pump}} \quad \text{..... (7)}$$

Where:

$P2, P1$: is the pressure at points 1 and 2 (kPa).

υ_1: is specific volume at point 1 (m^3/kg).

Finally, the system efficiency η_{ORC} is calculated as following:

$$\eta_{ORC} = \frac{\dot{W_t} - \dot{W_p}}{\dot{Q_e}} \quad \text{..... (8)}$$

So, the gross electric power of the ORC unit $(W_{e,gross})$ is calculated as following

$$W_{e,gross} = \eta_{ORC} Q_{HEX-ORC} \quad \text{..... (9)}$$

Where

$Q_{HEX-ORC}$ is the thermal power provided at the ORC unit evaporator from the storage tank.[9]

2.2. Thermal Absorption Chiller Modeling

With reference to the numbering system shown in figure 3, at point,[1] the solution is rich in refrigerant and a pump,[2] forces the liquid through a heat exchanger to the generator.[3] The temperature of the solution in the heat exchanger is increased. In the generator, thermal energy is added and the refrigerant boils off the solution. The refrigerant vapor,[7] flows to the condenser, where heat is rejected as the refrigerant condenses. The condensed liquid,[8] flows through a flow restrictor to the evaporator.[9] In the evaporator, the heat from the load evaporates the refrigerant, which flows back to the absorber.[10] A small portion of the refrigerant leaves the evaporator as liquid spillover.[11] At the generator exit,[4] the fluid consists of the absorbent–refrigerant solution, which is cooled in the heat exchanger. From points,[6-1] the solution absorbs refrigerant vapor from the evaporator and rejects heat through a heat exchanger.[8]

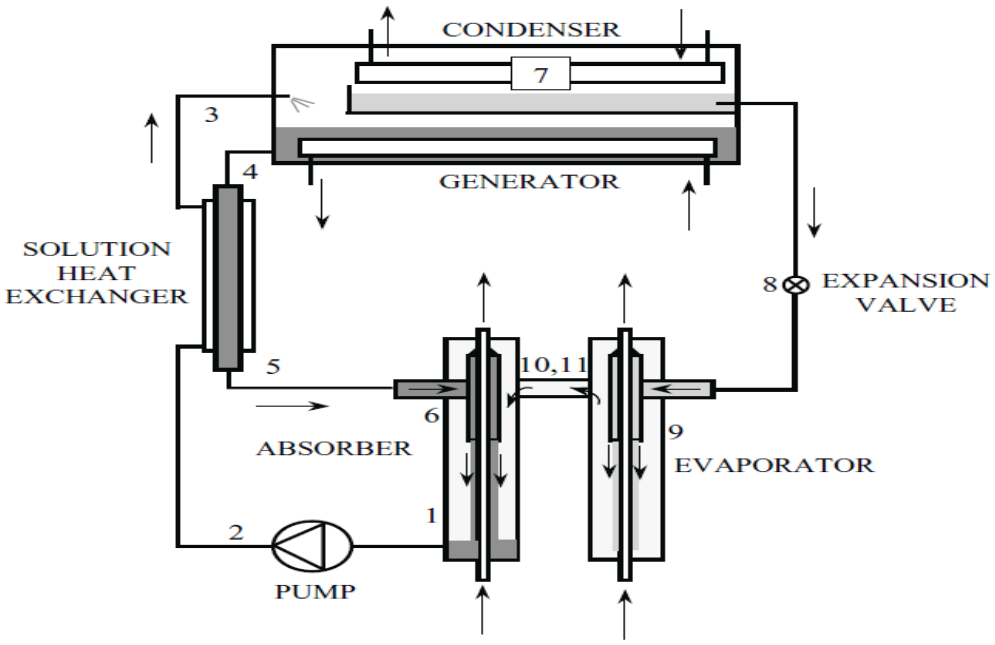

Fig. 3: Single effect, LiBr–water absorption cycle.[8]

To perform estimations of equipment sizing and performance evaluation of a single-effect LiBr–water absorption cooler, basic assumptions and input values must be considered. With reference to figure 3, the basic assumptions are

1. The steady state refrigerant is pure water.
2. There are no pressure changes except through the flow restrictors and the pump.
3. At points 1, 4, 8 and 11, there is only saturated liquid.
4. At point 10, there is only saturated vapor.
5. Flow restrictors are adiabatic.
6. The pump is isentropic.
7. There are no jacket heat losses.

Since, in the evaporator, the refrigerant is saturated water vapor and the temperature (T_{10}) is assumed, the saturation pressure at point 10 (P_{10}), as calculated from curve fit, and the enthalpy (h_{10}). Since, at point 11, the refrigerant is saturated liquid; its enthalpy can be calculated. The enthalpy at point 9 is determined from the throttling process applied to the refrigerant flow restrictor, which yields that $h_9=h_8$. To determine h_8, the pressure at this point must be determined. Since, at point 4, the solution mass fraction x_4 is an input value and the temperature at the saturated state was assumed, we can get the saturation pressure P_4 and h_4. Considering that the pressure at point 4 is the same as in point 8; then h_8 and h_9 can be obtained.

Once the enthalpy values at all ports connected to the evaporator are known, mass and energy balances can be applied to give the mass flow of the refrigerant and the evaporator heat transfer rate.

He mass balance on the evaporator is:

$$\dot{m}_9 = \dot{m}_{10} + \dot{m}_{11} \quad \text{..... (10)}$$

The energy balance on the evaporator is:

$$\dot{Q}_e = \dot{m}_{10}h_{10} + \dot{m}_{11}h_{11} - \dot{m}_9 h_9 \quad \text{..... (11)}$$

Where:

$\dot{m}_9, \dot{m}_{10}, \dot{m}_{11}$: The mass flow rate at points 9, 10, and 11 (kg/s).

h_9, h_{10}, h_{11}: The enthalpy at points 9, 10, and 11 (kJ/kg).

Since the evaporator output power $\dot{Q}_e$ and Liquid carryover from evaporator $\dot{m}_{11}$ as a percentage of $\dot{m}_{10}$ were assumed, the mass flow rates can be calculated.

Since the values of $\dot{m}_{10}$ and $\dot{m}_{11}$ are known, mass balances around the absorber give:

$$\dot{m}_1 = \dot{m}_{10} + \dot{m}_{11} + \dot{m}_6 \quad \text{.....(12)}$$

And $$x_1\dot{m}_1 = x_6\dot{m}_6 \quad \text{..... (13)}$$

The mass fractions x_1 and x_6 are inputs, and therefore $\dot{m}_1$ and $\dot{m}_6$ (mass flow rate at points 1 and 6 respectively) can be calculated. The heat transfer rate in the absorber can be determined from the enthalpy values at each of the connected state points. At point (1), the enthalpy (h_1) is determined from the input mass fraction x_1 is an input value and the assumption that the state is saturated liquid at the same pressure as the evaporator (P_{10}). The enthalpy value at point 6 (h_6) is determined from the throttling model, which gives $h_6 = h_5$.

The enthalpy at point 5 is not known but can be determined from the energy balance on the solution heat exchanger, assuming an adiabatic shell as follows:

$$\dot{m}_2h_2 + \dot{m}_4h_4 = \dot{m}_3h_3 + \dot{m}_5h_5 \quad \text{..... (14)}$$

Where:

$\dot{m}_2, \dot{m}_3, \dot{m}_4, \dot{m}_5$: The mass flow rate at points 2, 3, 4, and 5 (kg/s).

The temperature at point 3 is an input value, and since the mass fraction for points 1 to 3 is the same, the enthalpy at this point (h_3) is determined. Actually, the state at point 3 may be sub-cooled liquid. However, at the conditions of interest, the pressure has an insignificant effect on the enthalpy of the sub-cooled liquid, and the saturated value at the same temperature and mass fraction can be an adequate approximation. The enthalpy at point 2 is determined from an isentropic pump model.

The minimum work input (w) can, therefore, be obtained from

$$w = \dot{m}_1 \upsilon_1 (p_2 - p_1) \quad \text{……………………… ……………..……………. (15)}$$

Where:

$P2, P1$: is the pressure at points 1 and 2 (kPa).

υ_1: is specific volume at point 1 (m^3 /kg).

It is assumed that the specific volume (v, m^3/kg) of the liquid solution does not change appreciably from point (1)-(2). The specific volume of the liquid solution can be obtained from a curve fit.

Now, the unknown enthalpy value (h_5) at point 5can be obtained from the equation of the energy balance on the solution heat exchanger. The temperature at point 5 can also be determined from the enthalpy value.

Finally, the energy balance on the absorber is

$$\dot{Q}_a = \dot{m}_{10} h_{10} + \dot{m}_{11} h_{11} + \dot{m}_6 h_6 - \dot{m}_1 h_1 \text{…….………………………………….. (16)}$$

The heat input to the generator is determined from the energy balance, which is:

$$\dot{Q}_g = \dot{m}_4 h_4 + \dot{m}_7 h_7 - \dot{m}_3 h_3 \text{……………………..…………….……….. (17)}$$

The enthalpy at point 7 can be determined, since the temperature at this point is an input value. In general, the state at point 7 will be superheated water vapor, and the enthalpy can be determined once the pressure and temperature are known.

The condenser heat can be determined from an energy balance, which gives

$$\dot{Q}_c = \dot{m}_7 (h_7 - h_8) \quad \text{…………………………………………………. (18)}$$

Finally, the Coefficient of performance (COP) can be obtained by

$$COP = \frac{\dot{Q}_e}{\dot{Q}_g} \quad \text{..... (19)}$$

3. RESULTS

After dividing the stored thermal power into ORC and TDC at different percentages, ORC electric power (Wnet) and TDC cooling capacity ($\dot{Q}_e$) are calculated. Figure 4 shows the relation between the input thermal power of both ORC and TDC versus their outputs. With the reference to this figure, it was noticed that both ORC net output power and TDC cooling capacity increase with the increase of the input thermal power.

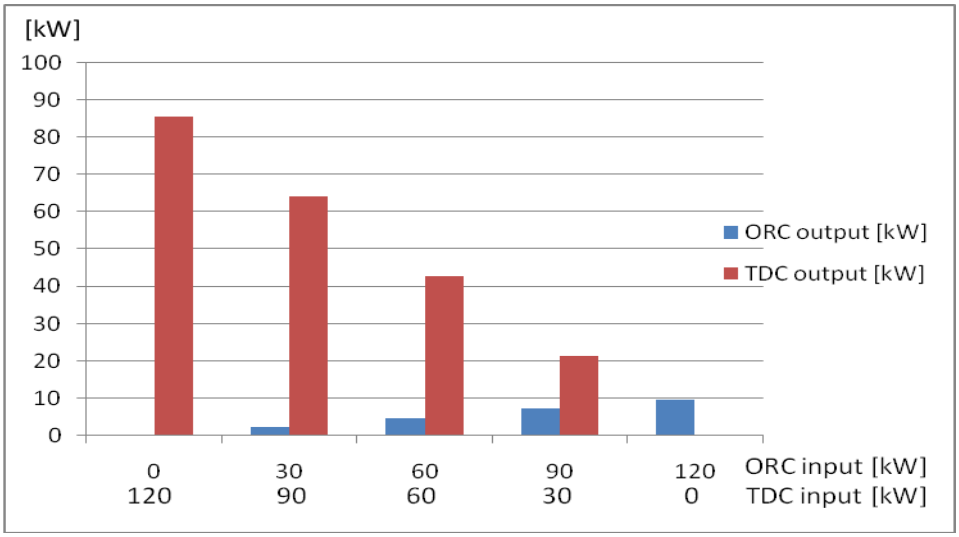

Fig. 4: ORC input thermal power vs. net output power and TDC input thermal power vs. cooling capacity.

3.1. Results of Organic Rankine Cycle

There are many parameters in the ORC which effect on the output electric power. Here, the effect of inlet hot oil temperature and hot oil mass flow rate on the input thermal power, net output power, and the ORC efficiency were investigated. Figure 5 shows the variation of ORC electric power output, inlet thermal power, and ORC efficiency versus the inlet hot oil temperature while the outlet hot oil temperature is/isn't constant. As seen in this figure, when the outlet hot oil temperature isn't constant, ORC output electric power is constant.

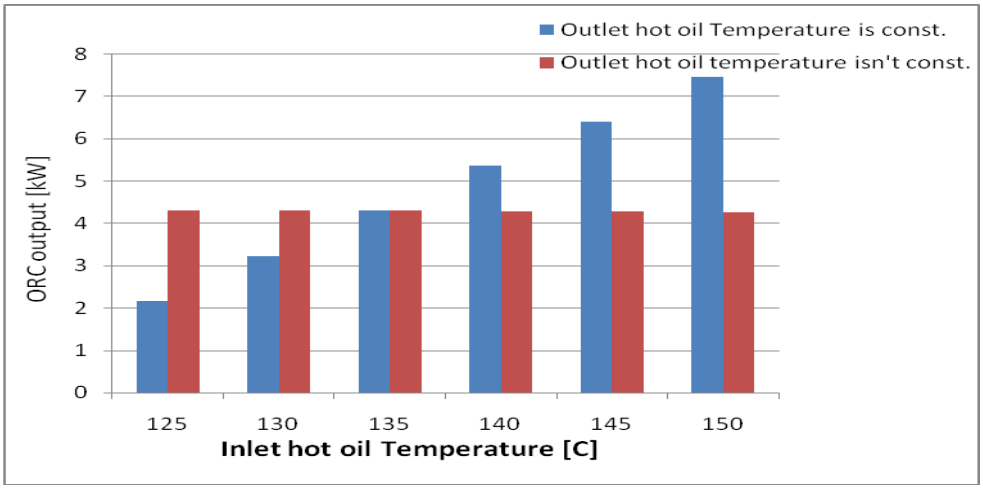

Fig. 5: Inlet hot oil temperature vs. ORC net output power.

As shown in figure 5, it is observed that when the inlet hot oil temperature increases, net electric power increases if the outlet hot oil temperature is constant and net electric power is constant if the outlet hot oil temperature increases. This is because when the inlet hot oil temperature increases and the outlet hot oil temperature is constant, the temperature difference increases, thus increasing the input thermal power, which increases net electric power. In the case of increasing the temperature of the outlet hot oil with the same increase in the inlet hot oil temperature, the input thermal power is constant and this lead to that net electric power is constant.

Figure 6 shows the effect of the mass flow rate of the hot oil (Msfo) on both the input thermal power and net output power. From this figure, it is clear that increasing mass flow rate increase both the input thermal power and net output power.

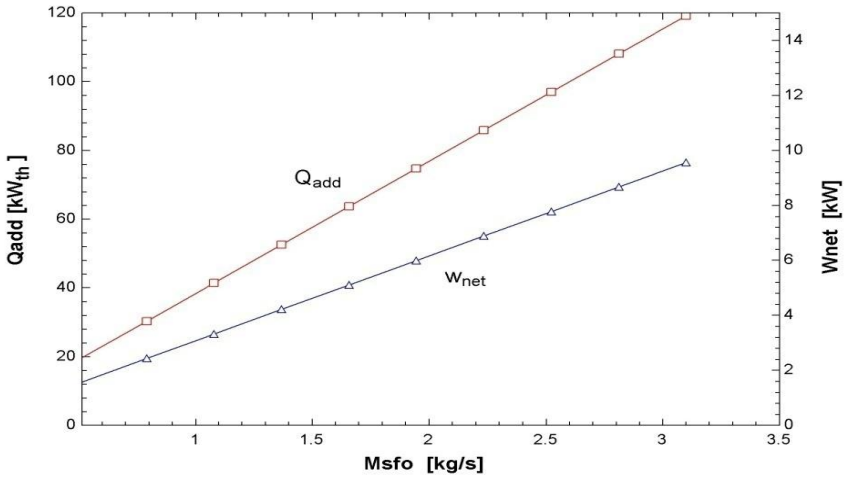

Fig. 6: Hot oil mass flow rate vs. input thermal power and net output power from ORC.

3.2. Results of Thermal Absorption Chiller

There are many parameters in the TDC modeling which effect on the COP like the effect of generator and evaporator temperatures. Increasing input thermal power is definitely offset by an increasing in the generator temperature. This statement is confirmed by figure 7 which illustrates the effect of the generator temperature on both the input thermal power and coefficient of performance.

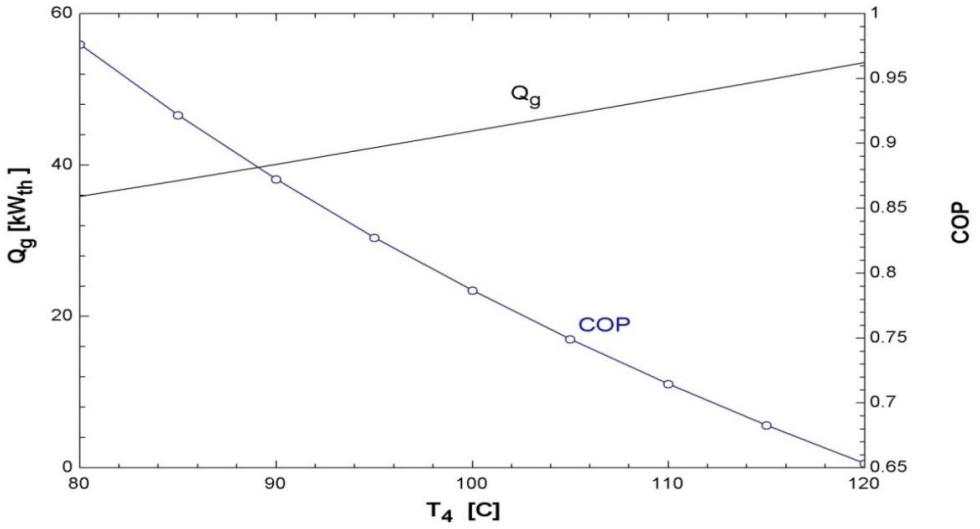

Fig. 7: Generator temperature vs. input thermal power and COP (TDC).

As shown from figure 7, with the generator temperature increasing, the input thermal power increases. This is because of in order to obtain a higher generator temperature; the input thermal power must be increased. Also, when the generator temperature is increased, the generator pressure is also increased, and this has the effect of lowering the COP of the unit, considering that the pressures and temperatures at other points of the unit are kept constant.

Figure 8 shows the effect of evaporator temperature on the required thermal power and the coefficient of performance of the system. It can be seen that required thermal power gradually decreases with the increase in evaporator temperature, thus increasing the coefficient of performance.

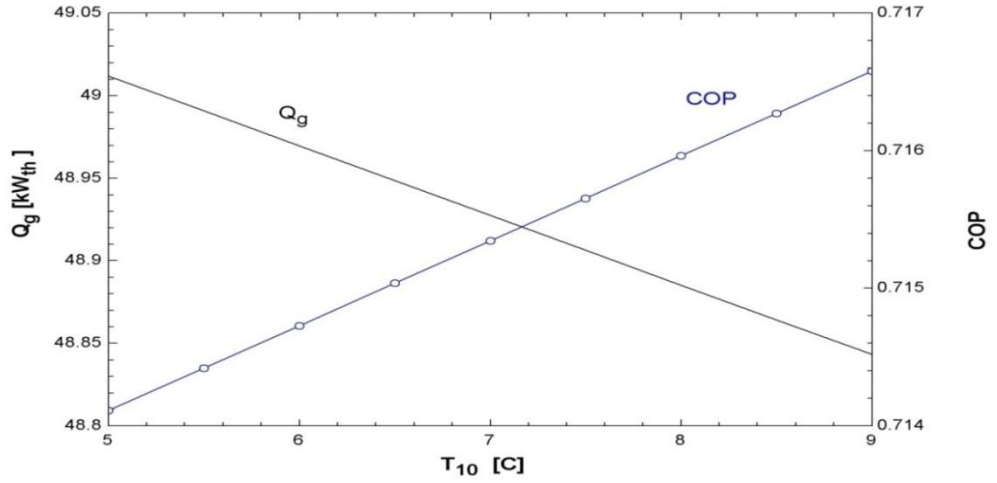

Fig. 8: Evaporator temperature vs. input thermal power and COP (TDC).

3.3. Analysis of kWh Cost

The study research plant cost is about 350,000 $. This cost is composed of about 140,000 $ for the solar field, 60,000 $ for the ORC, 30,000 $ for the chiller, and 120,000 $ for piping, pumps, cooling towers, control, and other auxiliary equipment.

At each case study the cost of electrical kWh and refrigerant kWh are calculated as follow:

ORC capital cost ($) = 60,000

TDC capital cost ($) = 30,000

Solar Field capital cost ($) = 140,000

Pumping, control, and piping cost ($) = 120,000

Operation and Maintenance cost ($) “assumed” = 15,000

Plant life time (yr) “assumed” n = 25

Total thermal stored power (kW) = 120

ORC daily operation (hr) = 7

TDC daily operation (hr) = 7

The annual electrical power generated can be obtained as

$$kwh_{elec,yr} = Wnet \cdot ORC_{hr} \cdot 365 \quad \text{..... (20)}$$

The annual refrigerant kW generated can be obtained as

$$kwh_{ref,yr} = \dot{Q}_e \cdot TDC_{hr} \cdot 365 \quad \text{..... (21)}$$

The using percentage of the stored thermal power for both ORC and TDC as follow,

$$X_{ORC} = \frac{Qadd}{120} \quad \text{..... (22)}$$

$$X_{TDC} = \frac{\dot{Q}_g}{120} \quad \text{..... (23)}$$

Finally, the cost of electrical kWh and refrigerant kWh can be obtained from eq. 24 and eq. 25.

$$kwh_{elec,cost} = \frac{ORC_{cost} + X_{ORC} \cdot (SF_{cost} + PC_{cost} + OM_{cost} \cdot n)}{kwh_{elec,yr} \cdot n} \quad \text{..... (24)}$$

$$kwh_{ref,cost} = \frac{TDC_{cost} + X_{TDC} \cdot (SF_{cost} + PC_{cost} + OM_{cost} \cdot n)}{kwh_{ref,yr} \cdot n} \quad \text{..... (25)}$$

Table 1: kWh cost values for both ORC and TDC at different cases.

% Input power for ORC	% Input power for TDC	ORC kWh cost [$/kWh]	TDC kWh cost [$/kWh]
25%	75%	1.423	0.1232
50%	50%	1.228	0.1269
75%	25%	1.163	0.1378
100%	0%	1.131	--
0%	100%	--	0.1214

From Table 1, it was found that when increasing the input thermal power for both ORC and TDC, the kWh cost decreases. Figure 9 shows the relation between the input thermal power and kWh cost for both ORC and TDC.

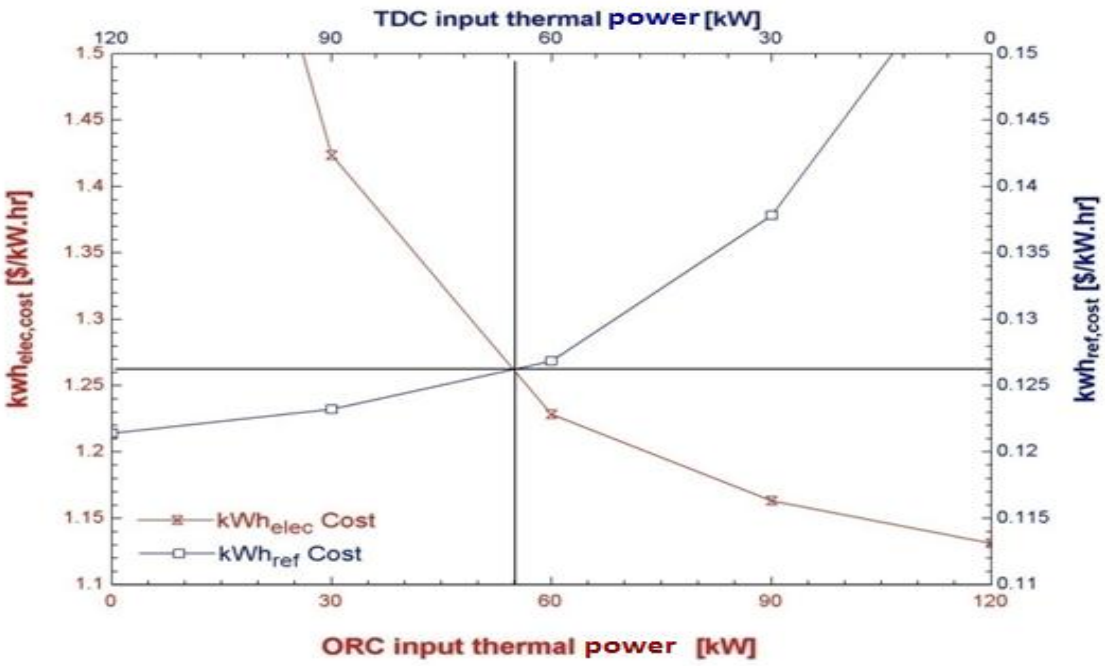

Fig. 9: Input thermal power vs. cost of kWh_elec. and cost of kWh_ref.

As shown in figure 9, the lowest price for ORC kWh is 1.131 $/kWh when 100% of the stored thermal power is used by ORC to generate electricity. Also, the lowest price for TDC kWh is 0.1214 $/kWh when 100% of the stored thermal power is directed to the TDC.

To compromise between both ORC and TDC, referring to figure 9, there is an intersection point between the two curves that corresponds to the best operating condition when about 45.83% from the stored thermal power is used for ORC and about 54.17% is used for TDC. In this case, the cost of electrical kWh from ORC is about 1.26$, while the cost of refrigerant kWh from TDC is about 0.126$.

4. CONCLUSIONS

Referring to the analysis of the results after simulate the proposed research plant which consists of solar collector field of 120 kW peak thermal capacity, thermal storage tank with 3 tons of therminol-66 oil, ORC of 8 kW nominal electric power production capacity, and TDC of 35 kW cooling capacity. Both ORC net output power and TDC cooling capacity increase with the increase of the input thermal power. When increasing the input thermal power for both ORC and TDC, the kWh cost decreases. The lowest price for ORC kWh is 1.131 $/kWh when 100% of the stored thermal power is used by ORC to generate electricity. Also, the lowest price for TDC kWh is 0.1214 $/kWh when 100% of the stored thermal power is directed to the TDC.

To compromise between both ORC and TDC, The best operating condition is obtained when about 45.83% from stored thermal power is used for ORC and 54.17% is used for TDC. In this case, the cost of electrical kWh from ORC is about 1.26 $, while the cost of refrigerant kWh from TDC is about 0.126 $.

REFERENCES

1. R. C. Bansal, T. S. Bhatti, and D. P. Kothari, "Bibliography on the application of induction generators in nonconventional energy systems", IEEE transactions on energy conversion, 2003; 18(3).
2. L. Chang and H.M. Kojabadi, "Review of interconnection standards for distributed power generation", Large Engineering Systems Conference on Power Engineering (LESCOPE' 02), 2002; 36 - 40.
3. Umberto Desideri, PietroEliaCampana, "Analysis and comparison between a concentrating solar and a photovoltaic power plant", Applied Energy, 2014; 113: 422–433.
4. Wisam Abed Kattea Al-Maliki, Falah Alobaid, Vitali Kez, Bernd Epple, "Modeling and dynamic simulation of a parabolic trough power plant", Journal of Process Control, 2016; 39: 123–138.
5. Monica Borunda, O.A. Jaramillo, R. Dorantes, Alberto Reyes, "Organic Rankine Cycle coupling with a Parabolic Trough Solar Power Plant for cogeneration and industrial processes", Renewable Energy, 2016; 86: 651-663.
6. Mustapha Merzouk, Nachida Kasbadji Merzouk, Said El Metenan, Omar Ketfi, "Performance of a Single Effect Solar Absorption Cooling System (Libr-H2O)", Energy Procedia, 2015; 74: 130 – 138.
7. Mohamed H. Ahmed, Mohamed A. Rady and Amr M. A. Amin, "Multi Applications of Small Scale Solar Power Plant Using Organic Rankine Cycle and Absorption Chiller", 2014.
8. G.A. Florides, S.A. Kalogirou, S.A. Tassou, L.C. Wrobel, "Design and construction of a LiBr–water absorption machine", Energy Conversion and Management, 2003; 44: 2483–2508.
9. M. Astolfi, L. Xodo, M. C. Romano, E. Macchi, Technical and economic analysis ofa solar-geothermal hybrid plant based on an Organic Rankine Cycle, 2010; 40: 58-68.

10. Mohamed Rady, Amr Amin, Mohamed Ahmed, "Conceptual Design of Small Scale Multi-Generation Concentrated Solar Plant for a Medical Center in Egypt", Energy Procedia, 2015; 83: 289 – 298.